Degradation Of Phenolic Compounds Using Synergetic Activated Carbon Blended Nanocomposite Catalysts Synthesized Via Thermal Combustion

Section A-Research paper

DEGRADATION OF PHENOLIC COMPOUNDS USING SYNERGETIC ACTIVATED CARBON BLENDED NANOCOMPOSITE CATALYSTS SYNTHESIZED VIA THERMAL COMBUSTION

P. S.Abitha[1*], S. Grace Victoria[2]

Abstract

In this paper, we detail the phenolic degradation assisted by pure and mixed photocatalysts of Activated Carbon (AC), Zinc Oxide (ZnO) and Copper Oxide (CuO). The photocatalysts are synthesized through a facile thermal combustion technique. X-ray Diffraction (XRD), Fourier Transform Infrared Spectroscopy (FTIR), Scanning Electron Microscopy (SEM) and UV- Visible Diffuse Reflectance Spectroscopy (UV-DRS) are employed to determine the crystallinity, morphology, phase formation and optical parameters of the prepared catalysts. The photocatalytic activity of the synthesized photo catalysts were tested using phenol degradation at various molar concentrations. Activated carbon was employed as a support for the photocatalytic degradation of dye molecules, in which the composite material demonstrated promising performance. When exposed to sunshine, the AC/ZnO/CuO photocatalyst achieved its highest level of phenol degradation efficiency (96%).

[1*]Research Scholar, Reg.Number: 20113282132011, Department of Physics & Research Centre, Women's Christian College, Nagercoil- 629001, Tamil Nadu, India

Email: [1*]abithafranklin@gmail.com

[2]Assistant Professor, Department of Physics & Research Centre, Women's Christian College, Nagercoil-629001, Tamil Nadu, India

(Affiliated to Manonmaniam Sundaranar University, Abishekapatti, Tirunelveli-627012, TamilNadu, India)

Eur. Chem. Bull. 2022, 11 (03), 586 – 598

586

Degradation Of Phenolic Compounds Using Synergetic Activated Carbon Blended Nanocomposite Catalysts Synthesized Via Thermal Combustion

Section A-Research paper

1. INTRODUCTION

Population explosion, climatic changes and industrial expansion have tremendously amplified the usage of water across the globe [1]. Water pollution is an exigent issue in the management of ecosystem[2] [3]. Dyes, organic compounds, heavy metals, pesticides, antibiotics and hormone drugs contaminate water bodies[4]. Phenol and phenolic compounds are one of the toughest perilous organic pollutants in water. The major sources of phenol are through discharges from industries of pulp, paper, pharma and pesticides [5] .Phenolic poisoning induce diseases such as cancer, kidney damage, development retardation, autoimmunity, extremely high endocrine disrupting potency, genotoxicity and even cause death [6, 7]. Taking the gravity of the danger into account, waste water treatment has garnered much attention. Various methods like coagulation, reverse osmosis, photo-degradation, chemical oxidation, membrane filtration, adsorption treatment, chemical precipitation, solvent extraction, ion exchange, nanofiltration, reverse osmosis, electrochemical techniques, ozonation and biosorption are employed for the removal of dyes in water bodies [8-13].

Photocatalytic treatment is one of the most effective dye removal method due to its high efficiency, nontoxicity, low cost and easy removal [14]. Metal Oxides are commonly used for photocatalytic applications. Oxides of Titanium, Zinc, Iron, Copper, and Cobalt are widely used in photocatalytic applications [14-17]. Zinc Oxide (ZnO) and Copper Oxide (CuO) have shown significant promise as low-cost, environmentally friendly and possessing high basicity and recyclability in waste water treatment approach. However, the major drawback encountered is low quantum efficiency due to inefficient visible light harvesting. To counter the hindrance of low efficiency, Activated Carbon (AC) is one of the most used adsorbents possessing high pollutant adsorption efficiency thus providing excellent catalytic support to the metal oxide photocatalysts. Significant amount of previous work has been reported for Sr/Ce/AC, Fe/TiO$_2$/AC, AC/TiO$_2$, ZnO/AC and W/TiO$_2$/AC etc. [18-20]. To the best of authors knowledge there is limited reports published for the phenolic degradation of ZnO/CuO incorporated activated carbon. Hence, in the present study, we blended Activated Carbon with ZnO/CuO using simple thermal combustion method. The synthesized composite material is characterized using XRD, FTIR, SEM, EDAX, UV-DRS. The photo catalytic activity was studied with phenol degradation using UV-VIS spectrophotometer.

2. MATERIALS AND METHODS

2.1. Materials and Chemicals
For the synthesis of the nanocomposites, Sigma Aldrich-obtained activated carbon (AC) was used as the support material. The precursors Zinc acetate (ZnC$_4$H$_6$O$_4$) and Copper acetate (Cu(CH$_3$COO)$_2$) were sourced from Sigma Aldrich. Sodium hydroxide (NaOH) was obtained from the Himedia process. Sigma Aldrich deionized water (H2O) was used as solvent to prepare solutions with precise concentrations. All the chemicals are used without any additional purification.

2.2 Method of Preparation
Here used Thermal combustion method for the preparation of nano composite. Combustion synthesis, often referred to as Auto-Spreading Elevated-Temperature Amalgamation (ASTA), represents an ingenious and cost-effective approach to produce nanocrystalline powders of remarkable purity and uniformity. In this process, an exothermic chemical reaction is ignited between reactants, commonly involving metal or metalloid powders and oxidizers, which generates an abundance of heat. This internal heat source sustains the reaction and elevates temperatures to levels conducive for synthesizing nanocrystalline materials with exceptional homogeneity and purity. Simultaneously, Solution Combustion Synthesis (SCS) emerges as a remarkably versatile procedure in materials science. It exhibits the capacity to facilitate the prosperous creation of an extensive variety of nano-scale ceramic materials. The core principle behind SCS involves the controlled combustion of a solution containing precursor compounds. This controlled combustion generates the requisite heat to initiate the desired chemical reactions, resulting in the formation of finely structured, nano-sized ceramic materials. The versatility of SCS lies in its ability to tailor reaction conditions, precursor choices, and reaction parameters, allowing for the precise engineering of a diverse spectrum of advanced ceramic materials with unique properties and applications.

Activated carbon with Zinc Oxide (AC ZnO)
About 1g of activated carbon is taken in mortar and about 0.5 g of Zinc acetate is added to it and grounded for 1 hr. The resulting mixture was transferred into the silica crucible and calcinated at a temperature of 450 °C for 1 hr. The resultant precipitate was noted as ACZnO.

Activated carbon with Copper Oxide (AC CuO)
About 1g of activated carbon is taken in mortar and about 0.5 g of Copper acetate is added to it and grounded for 1 hr. The resulting mixture was transferred into the silica crucible and calcinated at

Eur. Chem. Bull. 2022, 11 (03), 586 – 598

587

Degradation Of Phenolic Compounds Using Synergetic Activated Carbon Blended Nanocomposite Catalysts Synthesized Via Thermal Combustion

Section A-Research paper

a temperature of 450 °C for 1 hr. The resultant precipitate was noted as ACCuO.

Activated carbon with Zinc Oxide and Copper Oxide nanoparticles (AC-Zno/Cuo)

In a 250 ml round bottomed flask, 0.5M zinc acetate with 50ml of distilled water and 1M NaOH with 10 ml of distilled water was prepared followed by the addition of 2 grams of activated carbon. The mixture was stirred continuously for two hours. To this (0.2M, 0.4M, 0.6M, and 0.8M) copper acetate with 50 ml of distilled water was added in dropwise

for 1 hour and stirred. After 1 hour, the solution was filtered using ethanol and water until the precipitate become neutral. Finally the precipitate was washed and dried in hot air oven for 24 hrs at a temperature of 80°C. Then the resultant precipitate was sintered in 400°C for 2 hrs in muffle furnace. The resultant precipitate corresponding to various copper acetate concentration (0.2M, 0.4M, 0.6M, and 0.8M) are labeled as AC/ZnO/CuO #1, AC/ZnO/CuO #2, AC/ZnO/CuO #3 and AC/ZnO/CuO #4 respectively. The preparation of AC/ZnO/CuO composite was shown in fig.1.
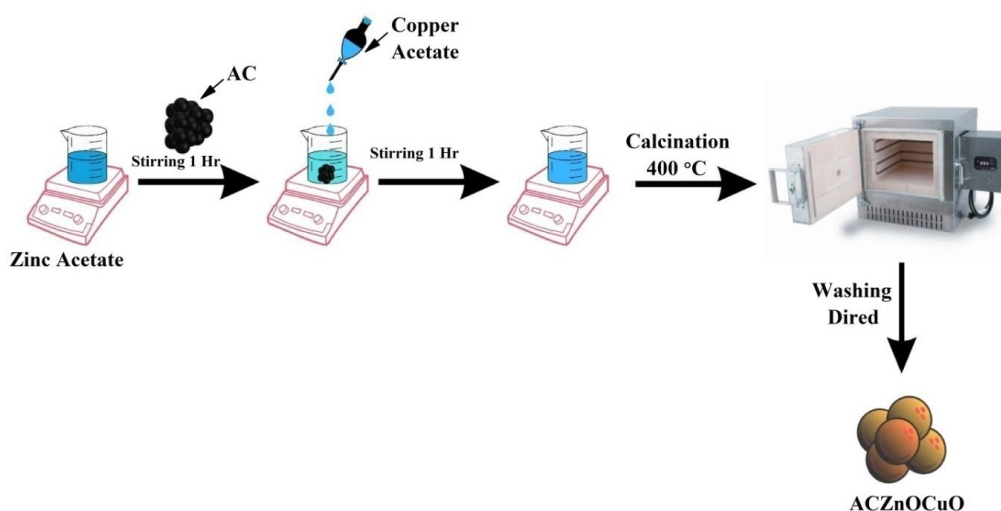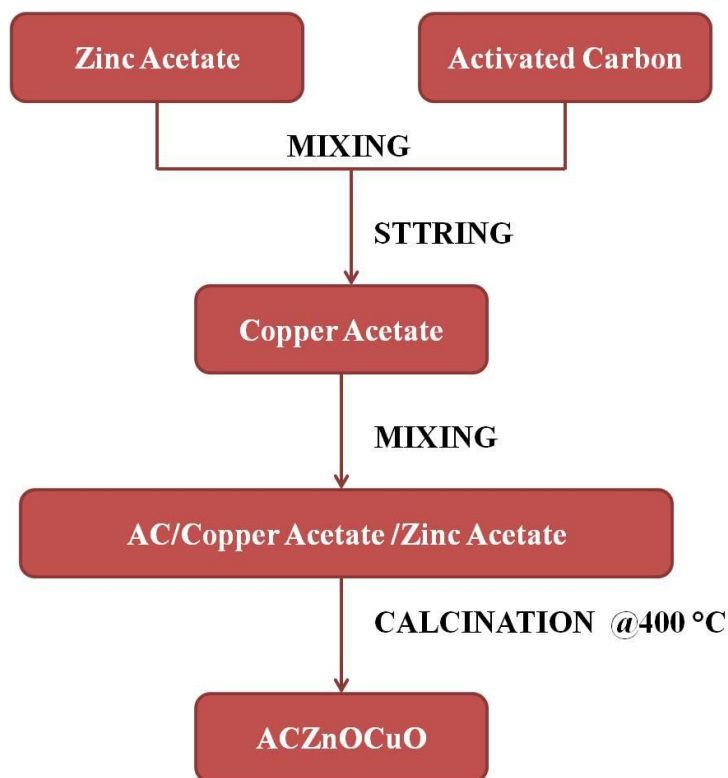

Fig.1. Schematic representation of ACZnOCuO Composite

Eur. Chem. Bull. 2022, 11 (03), 586 – 598

588

Degradation Of Phenolic Compounds Using Synergetic Activated Carbon Blended Nanocomposite Catalysts Synthesized Via Thermal Combustion

Section A-Research paper

2.3 Photocatalytic Degradation Experiment

Analysis of the photocatalytic degradation of phenol was studied using natural sunlight radiation. To initiate the reaction, 50 ml of phenol was poured into a 50 ml beaker. About 2 milligrams of photocatalyst was added to the phenol solution, which was then kept in the dark for two hours to determine the kinetics of adsorption and desorption. In a laboratory-constructed irradiation chamber, the solution was exposed to natural sunlight radiation. Then, aliquots of the solution were removed at 1 hour intervals, centrifuged and the rate of variation in phenol concentration during each photocatalytic decolorization run was monitored using a spectrophotometer. The percentage of pollution degradation was calculated using the formula [21]

$$\% \text{ Degradation} = (A_0 - A) / A_0 \times 100$$

Where: A_0 = initial absorbance of phenol at a specific wavelength

A = absorbance of phenol at the specific wavelength after a certain period of time

The percentage of degradation can be determined by measuring the absorbance of the phenol solution before and after the photocatalytic reaction by using the formula above. Higher the percentage of degradation, greater is the efficiency of the photocatalytic system in degrading phenol.

2.4 Material characterization

The X-ray diffraction analysis was performed on an X-ray diffractometer (sample stage 3071/xx) with copper target (λ =1.5405 AU) in theta and 2 theta scan mode. Fourier transform infrared spectroscopy (FTIR) (Thermo Nicolet FTIR spectrophotometer) was employed to investigate the chemical bonding in the powders of wavelength ranging from 4000 to 400 cm$^{-1.}$ The surface and compositional analysis were examined using SEM/EDAX (Joel 6390LA/ OXFORD XMX N) instrument for various magnifications. UV-VIS NIR Spectrophotometer is the analytical instrument used to measure the adsorption or transmission of light across a wide range of wavelengths.

3. RESULT AND DISCUSSION

3.1 Structural Elucidation by XRD

The X-ray diffraction (XRD) pattern obtained for the activated carbon sample reveals a broad peak within the range of 22-24°, indicative of the presence of amorphous carbon shown in figure 2(a). This amorphous morphology provides a greater surface area, allowing for more ionic species to adsorb into the activated carbon matrix.
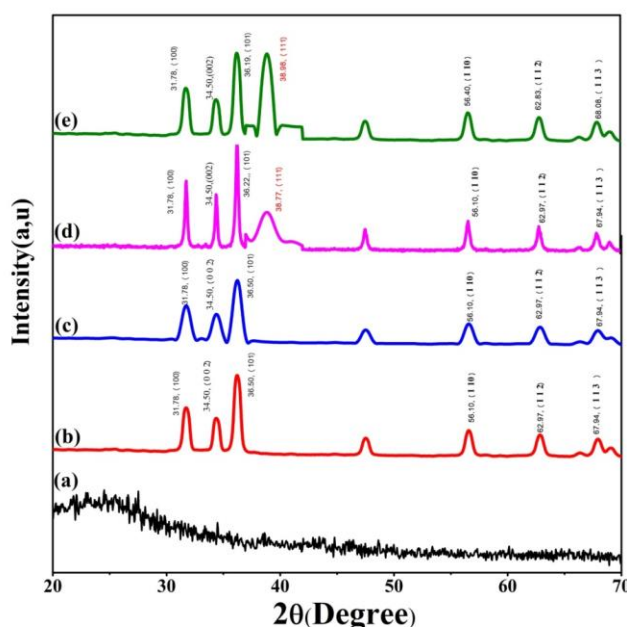

Fig.2. XRD Spectra of (a) AC (b) AC/ZnO/CuO#1 (c) AC/ZnO/CuO#2 (d) AC/ZnO/CuO#3 (e) AC/ZnO/CuO#4

The XRD analysis also confirms the existence of zinc oxide (ZnO) and copper oxide (CuO) phases within the composite. The ZnO phase is identified through its characteristic 2θ values of 32.15 (100), 35.25 (002), 58.10 (110) and 65.96 (112) as shown in figure 2(b)[JCPDS card no. 36-1451] [22, 23].

Eur. Chem. Bull. 2022, 11 (03), 586 – 598

589

Degradation Of Phenolic Compounds Using Synergetic Activated Carbon Blended Nanocomposite Catalysts Synthesized Via Thermal Combustion

Section A-Research paper

Similarly, the CuO phase is confirmed by the observed 2θ value of 38.59 (200) in figure (d and f) [JCPDS card no. 89-5896 [24]. Notably, the lattice parameters for the ZnO component in the CuO/ZnO nanocomposite deviate from standard values, indicating that the coupling between copper oxide and zinc oxide primarily occurs intra-granularly. This suggests that the two phases are intimately associated, leading to enhanced semiconductor coupling effects. The presence of ZnO/CuO over the activated carbon matrix in the AC/ZnO/CuO #3 nanocomposite is further supported by the peaks observed in the XRD pattern, confirming the successful synthesis of the photocatalytic material. It is worth noting that activated carbon is frequently utilized as a support for catalysts due to its high surface area and porous structure that can enhance the contact between the catalyst and reactants.

Table 1. Position of diffraction peaks (2 θ) of AC/ZnO/CuO photocatalyst

Position of diffraction peaks (2 θ)	Miller Indices (hkl)	JCPDS card no.
32.15 , 35.25 , 58.10 , and 65.96	(100), (002), (110) and (112)	36-1451 (ZnO)
38.92	(1 1 1)	89-5896 (CuO)

A. Phase formation by Fourier Transform Infrared Spectroscopy (FTIR)

The chemical skeleton and functional groups present in the AC and AC doped metal oxides are shown in Fig 3 (a-e). The O-H bond stretching vibration of the interlayer water molecules and hydroxyl groups responsible for the broad absorption band that was found between 3200 and 3500 cm^{-1} is evident in all the samples. A broad band centered about 585 cm^{-1} indicates the vibration caused by the Cu-O stretching band. The presence of metal carbonyl groups on the surface of the resulting nanoparticles can be deduced from the samples by looking for peaks in the region 1400–1600 cm^{-1} [25].The metal–oxygen (M–O) stretching mode can be identified based on the presence of a broad band in the range of 400–600 cm^{-1}.
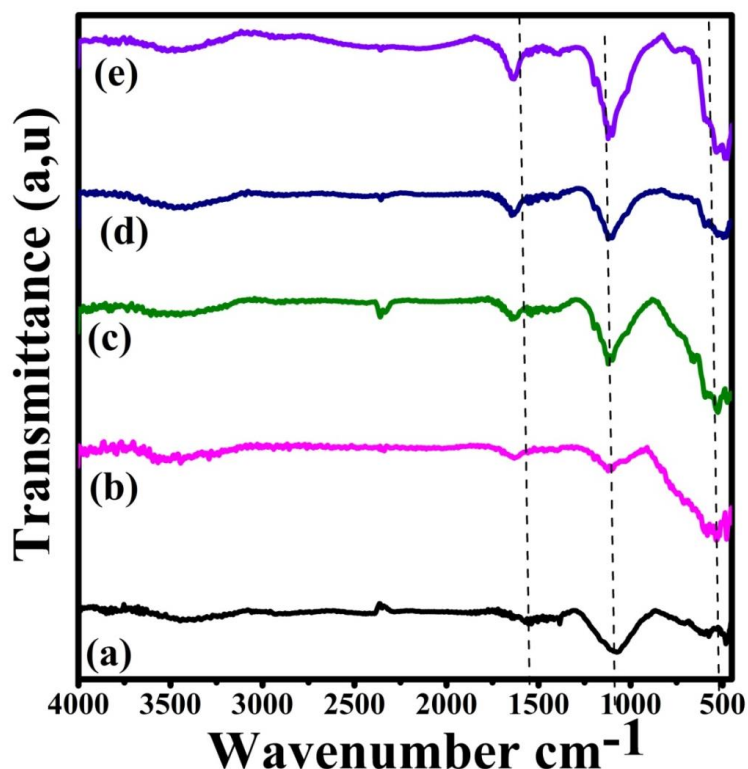

Fig.3. FTIR spectra of (a) AC (b) AC/ZnO/CuO#1, (c) AC/ZnO/CuO#2 (d) AC/ZnO/CuO#3 and (e) AC/ZnO/CuO#4

The formation of pure ZnO is verified by the presence of a peak at a wavelength of 460 cm^{-1} in Figure 3. This peak moves to wavelengths of 475, 510 and 540 cm^{-1} in (e) AC/ZnO/CuO #2 and (f) AC/ZnO/CuO #3 and (g) AC/ZnO/CuO#4, respectively, when the concentration of CuO is increased. These alterations are the result of a CuO crystal being inserted into ZnO nanoparticles.

Eur. Chem. Bull. 2022, 11 (03), 586 – 598

590

Degradation Of Phenolic Compounds Using Synergetic Activated Carbon Blended Nanocomposite Catalysts Synthesized Via Thermal Combustion

Section A-Research paper

B. Morphology examination by Scanning Electron Microscopy (SEM) and Purity Confirmation by Energy Dispersive Xray Spectroscopy (EDAX)
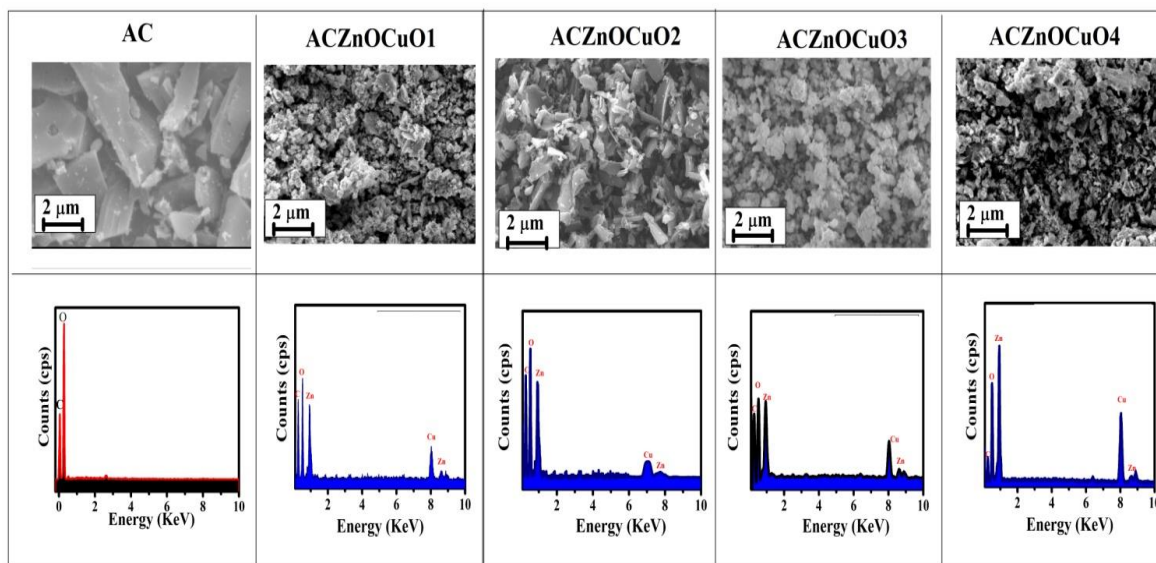

Fig.4. SEM and EDAX images of AC, AC/ZnO/CuO#1, AC/ZnO/CuO#2, AC/ZnO/CuO#3 and AC/ZnO/CuO#4.

Table.2. Elemental composition of AC/ZnO/CuO of various AC/ZnO/CuO photocatalyst

Elements Presents	Atomic Percentage (%)			
	AC/ZnO/CuO#1	AC/ZnO/CuO#2	AC/ZnO/CuO#3	AC/ZnO/CuO#4
C	53.62	35.9	34.7	38.08
O	36.29	37.8	36.6	38.90
Cu	7.91	20.62	21.24	21.08
Zn	2.18	5.68	7.46	1.94
Total	100	100	100	100

SEM pictures (Fig.4.) indicate clearly that The AC/ZnO/CuO composite exhibit an irregular and aggregated appearance. This observation indicates that ZnO and CuO effectively covered the entire surface of the ACZnOCuO sample. Energy Dispersive X-ray (EDX) analysis revealed that the composite primarily consisted of carbon, oxygen, zinc and copper. The deposition of CuO and ZnO occurred on the flake-like structure of activated carbon, leading to the formation of extended, aggregated particles that covered the pores [26]. Furthermore, the addition of activated carbon played a crucial role in preventing excessive agglomeration of ZnO and CuO. The carbon dopant acted as a bridging agent between the two cationic metal oxides, facilitating enhanced interaction and suppressing pore size distortion. Notably, the porous structure of the activated carbon material encapsulated the ZnO-CuO materials, effectively confining them within the pore volume.The incorporation of ZnO-CuO over activated carbon resulted in several benefits. Firstly, it significantly reduced electron-hole recombination and mitigated charge carrier loss, leading to enhanced photocatalytic activity of the composite. Moreover, the composite exhibited improved light harvesting efficiency, enabling better utilization of solar energy during photocatalytic reactions. Additionally, an increase in the copper content was found to correspond to a more prominent peak in the EDX analysis, indicating a higher concentration of copper in the composite [27]. However, the primary elemental components remained carbon, oxygen, zinc and copper. The conspicuous absence of contaminants in the sample indicated its purity further establishing the reliability and quality of the AC/ZnO/CuO composite.

3.4. Optical Studies (UV- Diffuse Reflectance Spectroscopy)

Eur. Chem. Bull. 2022, 11 (03), 586 – 598

591

Degradation Of Phenolic Compounds Using Synergetic Activated Carbon Blended Nanocomposite Catalysts Synthesized Via Thermal Combustion
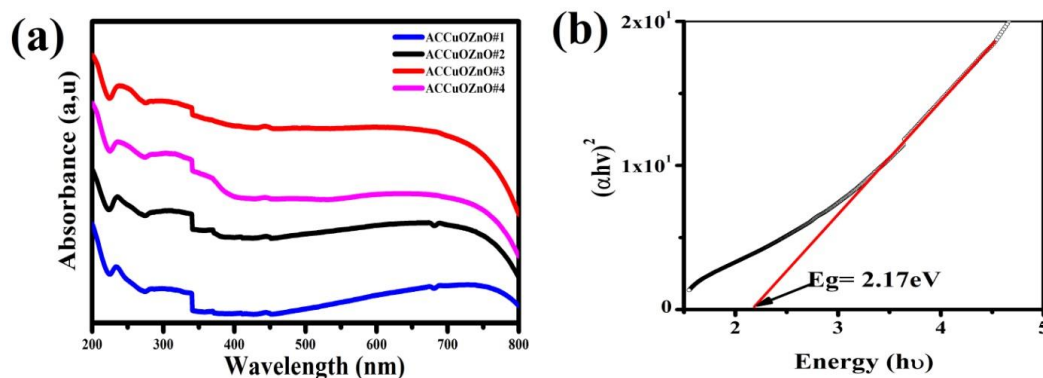
Section A-Research paper

Fig. 5 (a) UV–DRS Spectra for various AC/ZnO/CuO composite and (b) Tauc's plot of ACCuOZnO#3 composite.

The loading amount of CuO within the nanocomposites has a significant influence on their optical absorption characteristics, as evident from the DRS spectra presented in Figure 5 a. Notably, the ACCuOZnO#3 nanocomposites exhibit a distinct red shift towards higher wavelengths, accompanied by broad and prominent absorptions within the visible region. This concurrent behavior implies a reduction in the bandgap energy of the ACCuOZnO#3 composite. Conversely, the spectra of the other composites display comparatively lower absorption intensities within the visible range when compared to the ACCuOZnO#3 nanocomposites, indicating a discernible contrast between the two. To accurately determine the optical bandgap of the photocatalyst, the Tauc's relationship is employed as a reliable method, represented by Equation (2) [33]

$$(\alpha h\nu)^n = A(h\nu - E_g) \quad\ldots\ldots\ldots\ldots\ldots\ldots..(2)$$

In this equation, h denotes the Planck constant, ν represents the frequency of light, α signifies the absorption coefficient of the solid at a specific wavelength, and E_g denotes the bandgap energy. The relationship between these variables is visually illustrated in Figure 5.b. In this study, the ACCuOZnO#3 nanocomposite was found to possess band gap energy of 2.17 eV, which is lower than the values reported in previous literature[35]. This discrepancy suggests that the introduction of CuO and ZnO into the composite material has effectively altered its electronic structure, resulting in reduced bandgap energy. The lower bandgap energy indicates that the ACCuOZnO#3 nanocomposite is capable of absorbing a broader range of photons with lower energy, thereby extending its absorption into the visible spectrum.The observed decrease in bandgap energy could be attributed to several factors, including changes in the crystalline structure, composition and doping effects caused by the incorporation of

CuO and ZnO. These modifications may introduce additional energy levels within the bandgap, allowing for efficient absorption of visible light and enhancing the photocatalytic performance of the nanocomposite [37]. The decrease in bandgap energy observed in the ACCuOZnO#3 nanocomposites can be attributed to the increasing amounts of CuO incorporated into the material. The interaction between CuO and ZnO in these heterostructures play a crucial role in facilitating charge transfer processes. The presence of CuO and ZnO in close proximity results in an interfacial interaction that promotes the transfer of charges between the two materials. This charge transfer mechanism contributes to the modification of the electronic structure and, consequently, leads to a reduction in the bandgap energy of the ACCuOZnO#3 nanocomposites. The charge transfer process between CuO and ZnO can occur through various mechanisms, such as electron transfer or the formation of interfacial states. These processes allow for the redistribution of electronic states within the composite material, leading to a change in the energy band structure [34]. As a result, the bandgap energy is effectively lowered, enabling the nanocomposite to absorb photons with lower energy, including those in the visible range.The observed drop in bandgap energy due to the charge transfer between CuO and ZnO highlights the significance of the heterostructure formation and the synergistic effects between the two materials. This phenomenon opens up new possibilities for tailoring the bandgap energies of nanocomposites, offering potential applications in various optoelectronic and photocatalytic devices.

A. Photo catalytic studies
Degradation of phenol was carried out with the synthesized AC/ZnO/CuO nanocomposites using natural sunlight. The outcome of photocatalytic degradation study utilising different AC/ZnO/CuO composites is shown below. After contact duration

Eur. Chem. Bull. 2022, 11 (03), 586 – 598

592

Degradation Of Phenolic Compounds Using Synergetic Activated Carbon Blended Nanocomposite Catalysts Synthesized Via Thermal Combustion

Section A-Research paper

of 1 hour, the photocatalysts were found to have attained adsorption equilibrium and the AC composites showed comparable performance. This result demonstrates that factors other than activated carbon's surface area contributed significantly to the adsorption process upon addition of CuO, ZnO and other components to AC.
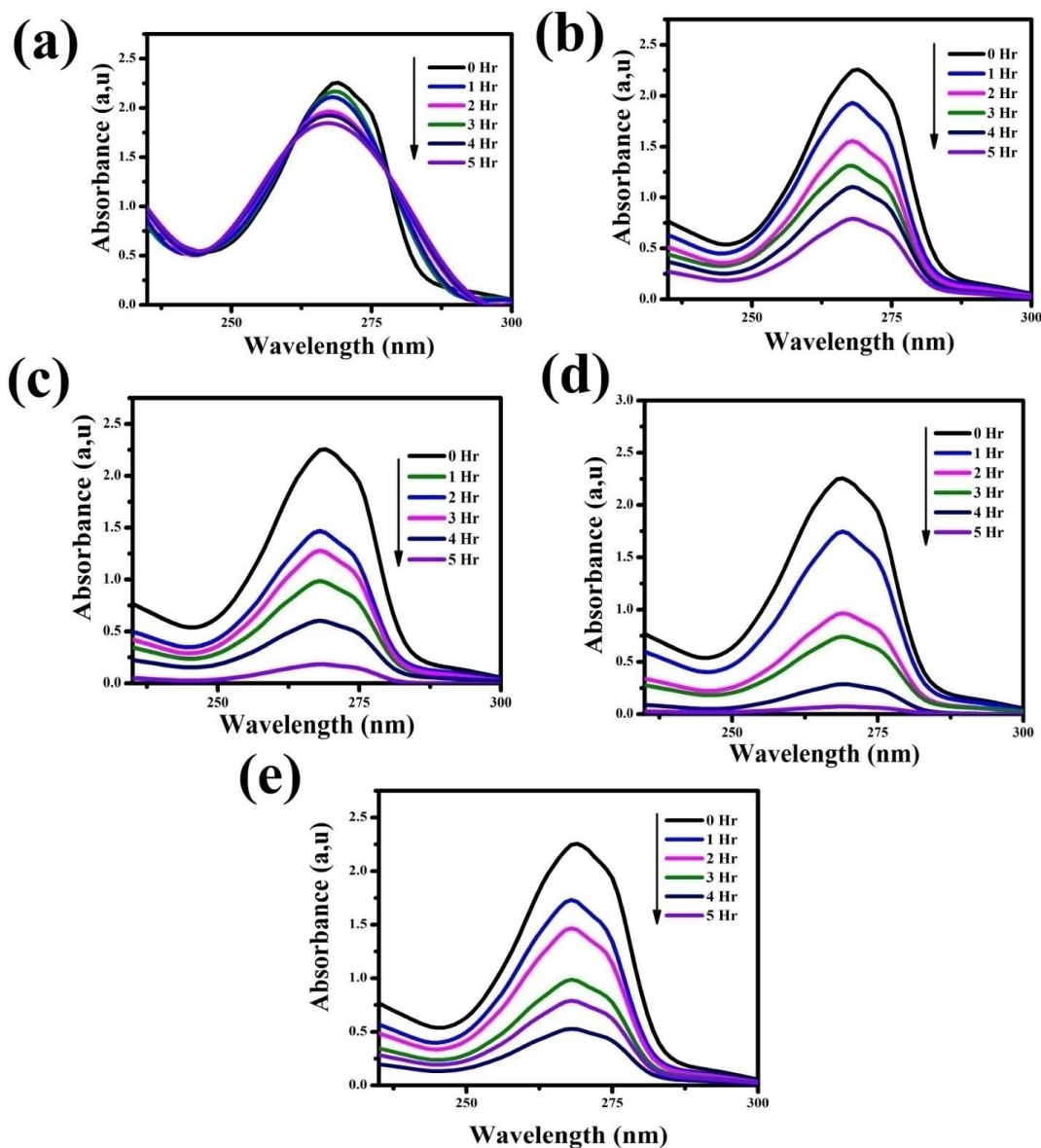

Fig. 6 UV Visible adsorption spectra (a) AC (b) AC/ZnO/CuO#1 (c) AC/ZnO/CuO#2 (d) AC/ZnO/CuO#3 and (e) AC/ZnO/CuO#4

The highest rate of phenol photodegradation was seen when exposed to natural sun light. After 5 hours of exposure to light, AC/ZnO/CuO#1 showed a photodegradation efficiency of 64%, whereas AC/ZnO/CuO#2 obtained 92%, AC/ZnO/CuO#3 attained 96%, and AC/ZnO/CuO#4 attained 76% and that of AC is just 18% is due to the surface adsorption only of AC matrix.. These findings show that AC/ZnO/CuO composites are effective photocatalysts for the degradation of phenol in the presence of sun radiation. Differences in photocatalyst composition, surface qualities and structural factors account for the observed range of photodegradation efficiencies among the various composites. Increased photocatalytic activity may be attributed to the inclusion of CuO and ZnO in the composites, which both improve light absorption and enable charge transfer processes [42, 44]. Achieving high photodegradation efficiency requires optimising the CuO and ZnO loading inside the AC matrix.

Eur. Chem. Bull. 2022, 11 (03), 586 – 598

593

Degradation Of Phenolic Compounds Using Synergetic Activated Carbon Blended Nanocomposite Catalysts Synthesized Via Thermal Combustion

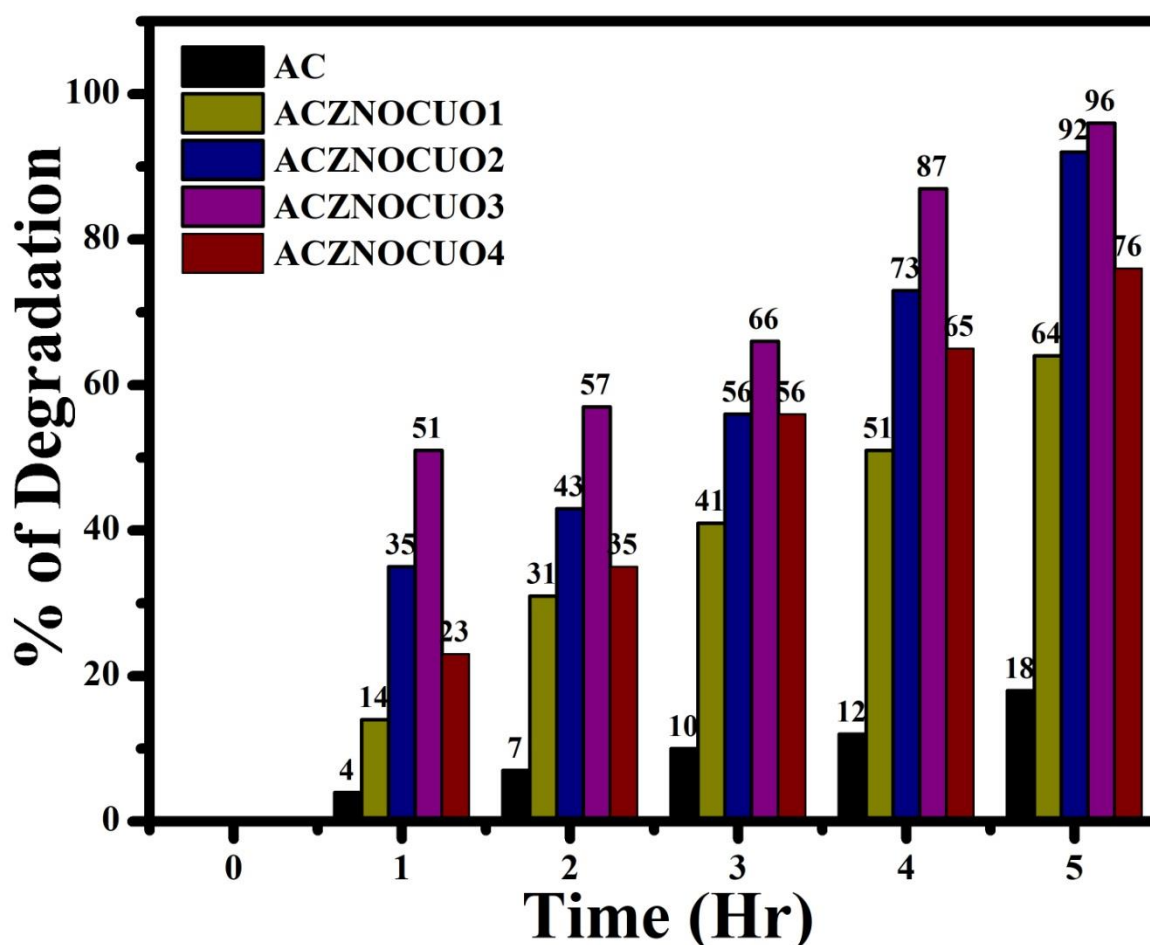*Section A-Research paper*

Fig. 7 Percentage of Phenol removal AC/ZnO/CuO#1, AC/ZnO/CuO #2, AC/ZnO/CuO #3 and AC/ZnO/CuO #4 against phenol at various time interval.

The mechanism of phenol photodegradation over the photocatalysts follow three steps. (1) Adsorption of organic pollutants onto the surface of the photocatalyst; (2) Photodegradation of phenol on the surface of the photocatalyst; and (3) Desorption of the end products from the surface of the photocatalyst. In the process of solar irradiation over binary metal oxide photocatalysts, electrons from the valence band (e-) of the semiconductor are promoted to the conduction band, which results in the generation of electron vacancies in the valence band. Thus, in Step (2), the electron vacancies (h+ VB) may have induced the oxidation of adsorbed phenol molecules on the surface of the photocatalyst, which directs the adsorbed water molecules with the consequent generation of hydroxyl radicals, •OH, and subsequently attacks the adsorbed phenol molecules that are affixed to the photocatalyst. The rate-dominant phase in the photodegradation of phenol is step 2, which may block the more rapid adsorption process that takes place on the active sites. During the process of irradiation, in addition to the formation of hydroxyl radicals, •OH, the photochemical formation of superoxide radical ion O2 • takes place. This is caused by the presence of O2 in the aqueous solution, and it serves as a precursor for many reactive species that are produced by photochemical reactions. The superoxide radical, also known as O2•, is an essential component in the production of the hydroxyl radical. This radical also prevents the recombination of the electron and hole pair that is present in the catalyst, which in turn speeds up the redox reaction [46-48]. In this way, photon-generated holes (h+ VB), photo-promoted electrons (e- CB), hydroxyl radicals (OH•), and superoxide ions (O2•) all take part in heterogeneous photocatalytic processes under circumstances that are thermodynamically favourable. They have the ability to break down organic molecules into intermediates, which can then be further broken down into carbon dioxide and water. The study of various photocatalyst over phenol degradation are tabulated in Table 3. The finding of the present work is also included.

Eur. Chem. Bull. 2022, 11 (03), 586 – 598

594

Table.3. Comparison study of various photocatalyst over phenol pollutant

S.No	Catalyst	Pollutant volume	Catalyst Dosage	Irradiation Source	Efficiency	Ref
	Cu-NiO)	100 ml	0.25 g	150 W high-pressure UV lamp	85.7% within 150 min.	[35]
	TiO2/Activated carbon (AC) and ZnO/AC	300 ml	0.1 g/l to 1 g/l	8.1 W UV lamp	85% 240 min	[36]
	(Fe/MWCNT/TiO2-A	200 ml	50 mg	Uv lamp	100% 180 min	[37]
	Fe-TiO2	50 ml phenol	0.2 g	UV Lamp, sun light, fluorescence light and dark place	7.8%, 12%, 7.5%, 6.8% and 5% obtained after 24 h	[38]
	AC	400 mL	1 g	high pressure mercury lamp (125 W)	80 % after 6 hours	**[39]**
	g-CN@CuO	350 mL	200 mg	500 W xenon lamp	97% for 120 min	[40]
	rGO/ZnO/TiO2	250 mL	100 mg	270.7 Cd lamps equipped	100% for 160 min	[41]
	AC/ZnO/CuO	**100 ml**	**2 mg**	**Natural sunlight**	**96% 300 min**	**Current work**

4. Conclusion

In this study, we examined the structural, morphological, o ptical and photocatalytic characteristics of thermally combusted AC/ZnO/CuO nanocomposites. We have confirmed the successful homogeneous incorporation of ZnO/CuO within the AC matrix using a variety of characterization techniques, including X-ray Diffraction (XRD), Fourier-Transform Infrared Spectroscopy (FTIR), Energy-Dispersive X-ray Spectroscopy (EDX), Scanning Electron Microscopy (SEM) and Diffuse Reflectance Spectrosopy. The findings of the evaluation of the photocatalytic activity of the AC/ZnO/CuO nanocomposites showed their astounding effectiveness in the phenol degradation process. The AC/ZnO/CuO nanocomposites had a remarkable phenol degradation rate of 96% after just 5 hours of exposure to natural sunshine. The remarkable photocatalytic activity of these nanocomposites demonstrates their promise for the effective eradication of environmental contaminants. Additionally, using AC as a support material for the photocatalysts has a number of benefits. Target pollutants may be more easily adsorbed on AC's stable and porous structure, which improves their interaction with the photocatalytic materials. The total effectiveness of the nanocomposites for pollutant removal is boosted by the synergistic interaction between ZnO/CuO and AC. In conclusion, the thermal combustion approach was used to create AC/ZnO/CuO nanocomposites that had high structural integrity, homogenous ZnO/CuO inclusion, and outstanding photocatalytic activity for phenol degradation. The nanocomposites become more capable of adsorption and interaction when AC is used as a support material, making them interesting candidates for the effective removal of environmental contaminants.

5. Reference

1. Subramanian, K., The crisis of consumption of natural resources. International Journal of Recent Innovations in Academic Research, 2018. **2**(4): p. 8-19.
2. Haseena, M., et al., Water pollution and human health. Environmental Risk Assessment and Remediation, 2017. **1**(3).
3. Inyinbor Adejumoke, A., et al., Water pollution: effects, prevention, and climatic impact. Water Challenges of an Urbanizing World, 2018. **33**: p. 33-47.
4. !!! INVALID CITATION !!!
5. Anku, W.W., M.A. Mamo, and P.P. Govender, Phenolic compounds in water: sources, reactivity, toxicity and treatment methods. Phenolic compounds-natural sources, importance and applications, 2017: p. 419-443.
6. Mainali, K., Phenolic compounds contaminants in water: A glance. Curr. Trends Civil Struct. Eng, 2020. **4**: p. 1-3.

Degradation Of Phenolic Compounds Using Synergetic Activated Carbon Blended Nanocomposite Catalysts Synthesized Via Thermal Combustion

Section A-Research paper

7. Hammam, A., et al., Toxicity, Mutagenicity and carcinogenicity of phenols and phenolic compounds on human and living organisms [A Review]. Advances in environmental biology, 2015. **9**(8): p. 38-49.

8. Villegas, L.G.C., et al., A short review of techniques for phenol removal from wastewater. Current Pollution Reports, 2016. **2**(3): p. 157-167.

9. Mohammadi, S., et al., Phenol removal from industrial wastewaters: a short review. Desalination and Water Treatment, 2015. **53**(8): p. 2215-2234.

10. Raza, W., et al., Removal of phenolic compounds from industrial waste water based on membrane-based technologies. Journal of industrial and engineering chemistry, 2019. **71**: p. 1-18.

11. Akbal, F. and A. Nur Onar, Photocatalytic degradation of phenol. Environmental monitoring and assessment, 2003. **83**(3): p. 295-302.

12. Pradeep, N., et al., Biological removal of phenol from wastewaters: a mini review. Applied Water Science, 2015. **5**(2): p. 105-112.

13. Chedeville, O., M. Debacq, and C. Porte, Removal of phenolic compounds present in olive mill wastewaters by ozonation. Desalination, 2009. **249**(2): p. 865-869.

14. Intarasuwan, K., et al., Photocatalytic dye degradation by ZnO nanoparticles prepared from X2C2O4 (X= H, Na and NH4) and the cytotoxicity of the treated dye solutions. Separation and Purification Technology, 2017. **177**: p. 304-312.

15. Hayat, K., et al., Nano ZnO synthesis by modified sol gel method and its application in heterogeneous photocatalytic removal of phenol from water. Applied Catalysis A: General, 2011. **393**(1-2): p. 122-129.

16. Zhang, Y., Y. Zhang, and J. Tan, Novel magnetically separable AgCl/iron oxide composites with enhanced photocatalytic activity driven by visible light. Journal of alloys and compounds, 2013. **574**: p. 383-390.

17. Al-Hamdi, A.M., et al., Efficient photocatalytic degradation of phenol in aqueous solution by SnO2: Sb nanoparticles. Applied Surface Science, 2016. **370**: p. 229-236.

18. Li, Y., et al., CuO particles and plates: synthesis and gas-sensor application. Materials Research Bulletin, 2008. **43**(8-9): p. 2380-2385.

19. Zhang, Q., et al., CuO nanostructures: synthesis, characterization, growth mechanisms, fundamental properties, and applications. Progress in Materials Science, 2014. **60**: p. 208-337.

20. Verma, N. and N. Kumar, Synthesis and biomedical applications of copper oxide nanoparticles: an expanding horizon. ACS biomaterials science & engineering, 2019. **5**(3): p. 1170-1188.

21. Srivastava, V., D. Gusain, and Y.C. Sharma, Synthesis, characterization and application of zinc oxide nanoparticles (n-ZnO). Ceramics International, 2013. **39**(8): p. 9803-9808.

22. Vaseem, M., A. Umar, and Y.-B. Hahn, ZnO nanoparticles: growth, properties, and applications. Metal oxide nanostructures and their applications, 2010. **5**(1): p. 10-20.

23. Shi, L.-E., et al., Synthesis, antibacterial activity, antibacterial mechanism and food applications of ZnO nanoparticles: a review. Food Additives & Contaminants: Part A, 2014. **31**(2): p. 173-186.

24. Sharma, G., et al., Highly efficient Sr/Ce/activated carbon bimetallic nanocomposite for photoinduced degradation of rhodamine B. Catalysis Today, 2019. **335**: p. 437-451.

25. Zhou, J., et al. Enhanced photocatalytic activity of Fe-doped TiO2 coated on N-doped activated carbon composites for photocatalytic degradation of dyeing wastewater. in AIP Conference Proceedings. 2017. AIP Publishing LLC.

26. Lam, S.-M., J.-C. Sin, and A.R. Mohamed, Parameter effect on photocatalytic degradation of phenol using TiO2-P25/activated carbon (AC). Korean Journal of Chemical Engineering, 2010. **27**(4): p. 1109-1116.

27. Sakthivel, S., et al., Solar photocatalytic degradation of azo dye: comparison of photocatalytic efficiency of ZnO and TiO2. Solar energy materials and solar cells, 2003. **77**(1): p. 65-82.

28. Khoshhesab, Z.M., M. Sarfaraz, and M.A. Asadabad, Preparation of ZnO nanostructures by chemical precipitation method. Synthesis and Reactivity in Inorganic, Metal-Organic, and Nano-Metal Chemistry, 2011. **41**(7): p. 814-819.

29. Priya, D.D., et al., Aerva lanata-mediated bio-treated production of copper oxide nanoparticles, optimization by BBD–RSM method and it behaviour against water related mosquito. Applied Nanoscience, 2021. **11**(1): p. 207-216.

30. Habibi, M.H. and B. Karimi, Application of impregnation combustion method for fabrication of nanostructure CuO/ZnO composite oxide: XRD, FESEM, DRS and FTIR study. Journal of Industrial and

Eur. Chem. Bull. 2022, 11 (03), 586 – 598

596

Degradation Of Phenolic Compounds Using Synergetic Activated Carbon Blended Nanocomposite Catalysts Synthesized Via Thermal Combustion

Section A-Research paper

Engineering Chemistry, 2014. **20**(4): p. 1566-1570.

31. Peri, J.B. and R.B. Hannan, Surface hydroxyl groups on γ-alumina1. The Journal of Physical Chemistry, 1960. **64**(10): p. 1526-1530.

32. Kendix, E., et al., Far infrared and Raman spectroscopy analysis of inorganic pigments. Journal of Raman Spectroscopy: An International Journal for Original Work in all Aspects of Raman Spectroscopy, Including Higher Order Processes, and also Brillouin and Rayleigh Scattering, 2008. **39**(8): p. 1104-1112.

33. Aghaei, M., S. Sajjadi, and A.H. Keihan, Sono-coprecipitation synthesis of ZnO/CuO nanophotocatalyst for removal of parathion from wastewater. Environmental Science and Pollution Research, 2020. **27**(11): p. 11541-11553.

34. Hitkari, G., S. Singh, and G. Pandey, Structural, optical and photocatalytic study of ZnO and ZnO–ZnS synthesized by chemical method. Nano-Structures & Nano-Objects, 2017. **12**: p. 1-9.

35. Melo, R., et al., Magnetic ferrites synthesised using the microwave-hydrothermal method. Journal of Magnetism and Magnetic Materials, 2015. **381**: p. 109-115.

36. Parvathiraja, C. and S. Shailajha, Plasmonic core–shell nanoparticles of Ag@ TiO2 for photocatalytic degradation of Rhodamine B. Applied Nanoscience, 2022: p. 1-16.

37. Zhou, N., et al., Plasmon-enhanced light harvesting: applications in enhanced photocatalysis, photodynamic therapy and photovoltaics. Rsc Advances, 2015. **5**(37): p. 29076-29097.

38. Jubu, P.R., et al., Dispensability of the conventional Tauc's plot for accurate bandgap determination from UV–vis optical diffuse reflectance data. Results in Optics, 2022. **9**: p. 100273.

39. Shinde, R.S., et al., Synthesis and characterization of ZnO/CuO nanocomposites as an effective photocatalyst and gas sensor for environmental remediation. Journal of Inorganic and Organometallic Polymers and Materials, 2022: p. 1-22.

40. Thatikayala, D. and B. Min, Ginkgo leaves extract-assisted synthesis of ZnO/CuO nanocrystals for efficient UV-induced photodegradation of organic dyes and antibacterial activity. Journal of Materials Science: Materials in Electronics, 2021. **32**(13): p. 17154-17169.

41. Albadarin, N.A., et al., Tunable morphology and band gap alteration of CuO-ZnO nanostructures based photocathode for solar photoelectrochemical cells. Materials Research Express, 2020. **7**(12): p. 125010.

42. Hussain, M.K., et al., Enhanced visible light-driven photocatalytic activity and stability of novel ternary ZnO/CuO/MoO3 nanorods for the degradation of rhodamine B and alizarin yellow. Materials Science in Semiconductor Processing, 2023. **155**: p. 107261.

43. Malwal, D. and P. Gopinath, CuO-ZnO Nanosheets with p–n Heterojunction for Enhanced Visible Light Mediated Photocatalytic Activity. ChemistrySelect, 2017. **2**(17): p. 4866-4873.

44. Yu, J., et al., Photogenerated electron reservoir in hetero-p–n CuO–ZnO nanocomposite device for visible-light-driven photocatalytic reduction of aqueous Cr (VI). Journal of Materials Chemistry A, 2015. **3**(3): p. 1199-1207.

45. El-Alami, W., et al., Efect of TiF surface interaction on the photocatalytic degradation of phenol, aniline and formic acid. Journal of Photochemistry and Photobiology A: Chemistry, 2017. **348**: p. 139-149.

46. Wang, J. and S. Wang, Reactive species in advanced oxidation processes: Formation, identification and reaction mechanism. Chemical Engineering Journal, 2020. **401**: p. 126158.

47. Lim, J., et al., Visible light sensitized production of hydroxyl radicals using fullerol as an electron-transfer mediator. Environmental Science & Technology, 2016. **50**(19): p. 10545-10553.

48. Ma, J., et al., Kinetic consideration of photochemical formation and decay of superoxide radical in dissolved organic matter solutions. Environmental Science & Technology, 2020. **54**(6): p. 3199-3208.

49. Ethiraj, A.S., et al., Photocatalytic performance of a novel semiconductor nanocatalyst: Copper doped nickel oxide for phenol degradation. Materials Chemistry and Physics, 2020. **242**: p. 122520.

50. Lee, H., et al., Phenol degradation catalyzed by metal oxide supported porous carbon matrix under UV irradiation. Journal of Water Process Engineering, 2019. **31**: p. 100869.

51. Marques, J.O., et al., Synthesis, characterization and enhanced photocatalytic activity of iron oxide/carbon nanotube/Ag-doped TiO 2 nanocomposites. Journal of the Brazilian Chemical Society, 2017. **28**: p. 2301-2312.

52. Shawabkeh, R.A., O.A. Khashman, and G. Bisharat, Photocatalytic degradation of phenol using Fe-TiO2 by different illumination sources. International Journal of Chemistry, 2010. **2**(2): p. 10-18.

Eur. Chem. Bull. 2022, 11 (03), 586 – 598

597

Degradation Of Phenolic Compounds Using Synergetic Activated Carbon Blended Nanocomposite Catalysts Synthesized Via Thermal Combustion

Section A-Research paper

53. Velasco, L.F., J.B. Parra, and C.O. Ania, Role of activated carbon features on the photocatalytic degradation of phenol. Applied Surface Science, 2010. **256**(17): p. 5254-5258.

54. Baishnisha, A., et al., Synthesis of highly efficient g-CN@ CuO nanocomposite for photocatalytic degradation of phenol under visible light. Journal of Alloys and Compounds, 2021. **886**: p. 161167.

55. Hayati, F., et al., Photocatalytic decontamination of phenol and petrochemical wastewater through ZnO/TiO 2 decorated on reduced graphene oxide nanocomposite: influential operating factors, mechanism, and electrical energy consumption. RSC advances, 2018. **8**(70): p. 40035-40053.

Eur. Chem. Bull. 2022, 11 (03), 586 – 598

598